IJCRT.ORG

ISSN: 2320-2882



INTERNATIONAL JOURNAL OF CREATIVE RESEARCH THOUGHTS (IJCRT)

An International Open Access, Peer-reviewed, Refereed Journal

APPLICATION OF Cd_{1-x}Mn_xS DILUTE MAGNETIC SEMICONDUCTOR IN PHOTO ELECTROCHEMICAL CELLS

S.V.Borse Dept.of Physics, S.S.V.P.S's ASC College, Shindkheda (M.S.) 425406

Abstract

CdMnS is an important class of dilute magnetic semiconductor material. It is reported that the CdMnS thin film have been used in photoelectrochemical cell. CdMnS dilute magnetic semiconductor thin films are synthesized on both glass and stainless steel substrates using a chemical bath deposition method CBD. The deposition parameters such as growth temperature, time, pH of bath solution, concentrations of precursor, etc., were optimized to obtain device grade and good oriented polycrystalline films. The layer thickness was found to be dependent on Mn^{2+} concentration. Composition of the as-grown films was determined by an EDAX technique. The electrochemical cells were fabricated by using the as deposited films of CdMnS of different composition as the active photoelectrodes, an electrolyte and a counter electrode. The cells were then characterized for their dark and illumination properties. different cell parameters such as Voc,Isc, FF, Rs,Rsh, η , nd and ΦB were determined from these experiment and the cell performance has been assess with a reference of Mn^{2+} concentration in CdS. A remarkable improvement in performance has been found for a cell with electrode of composition x = 0.1.

Key Words: Cd_{1-x}Mn_xS Magnetic semiconductor, DMS, Photoelectrochemical cell, Magnetic properties, fill factor.

1. Introduction:

In past few decades the Ternary alloy materials have been drawing an attention in the researcher's community because of easily tunable basic material properties such as energy gap, lattice constants and the effective mass, only by changing the elemental materials composition. Diluted magnetic semiconductors DMS are potential high performing candidates and are II-VI, IV-VI, II-V and III-V compounds in which a considerable numbers of nonmagnetic ions (e.g. Mn2+, Fe2+, Co2+) gives a variety of collaborative effects which are not seen in nonmagnetic semiconductors, due to spin-spin exchange interaction [1–5]. These materials, II-VI and IV-VI compounds, have the general configuration of type $AII_{1-x}B_xC_{IV}$ [where $AII_{1-x}=(Cd, Zn, Hg)$, $B_x=$ magnetic ions (Mn, Fe, Co) and $C_{IV}=(S, Se, Te)$] and have been extensively studied assigning to the semiconducting magnetic structures of the selenides, and tellurides; sulphides being less investigated [6,7]. Among DMS studied, Mn-contain DMS's can be grown over a wide range of composition than the others and due to their tunable lattice parameters and energy gaps, these Mn- contain alloys are outstanding candidates for preparation of quantum wells and super lattices [8,9]. Our objective is to synthesize a number of different composition of $Cd_{1-x}Mn_xS$ DMS materials under optimized conditions for application in electrochemical photovoltaic cell demonstrating that CdMnS is a potential candidate for optoelectronic applications, although it has been rarely studied in literature.

2. Experimental:

2.1. Materials synthesis:

The number of $Cd_{1-x}Mn_x$ S thin films of various composition $x = (0 \le x \le 0.5)$ were deposited onto well cleaned glass and stainless steel substrates by a chemical bath deposition method [10-13]. The chemical reagents used are cadmium sulphate, manganese sulphate, thiourea, liquid ammonia and Triethanolamine. All these chemicals are of AR grade from Merck and Loba chem. For deposition, hydrolyzed solutions of cadmium sulphate (at 1 M concentration), manganese sulphate (1 M) and thiourea (1 M) in stoichiometric proportions were prepared and placed in a 250 ml glass beaker. Triethanolamine (TEA) and liquid ammonia (NH3) were added into the reaction container as the complexing agent. For different compositions of films prepared, the film stoichiometry was controlled by controlling the ion concentration volumes of the basic three reactants. The cleaned glass and stainless steel substrates were mounted in a substrate holder. The substrate holder rotated in the reaction bath mixture by using a constant speed gear motor. This helps a homogeneous and continuous mechanical stirring of the solution mixture .in the reaction bath. To obtain good quality films, The amount of complexing agents was optimized. The deposition temperature, time, pH and speed of the substrate rotation were optimized. The final thicknesses of these as-deposited films were measured using an interference technique. The microscopic study were observed through a scanning electron microscope, JOEL-JSM 5600 (Bruker Instrument analytical limited 2000). Elemental composition of the films material in thin films is calculated by energy dispersive X-ray analysis JOEL-JSM 5600 (Bruker Instrument analytical limited 2000) (EDAX).

2.2. Photoelectrochemical cell fabrication:

An electrochemical photovoltaic cell is fabricated by using these films as one of the photoelectrodes. A polysulfide redox couple which is the pair of chemical species, an oxidized and a reduced form, that participate in a redox reaction involving polysulfides is used as electrolyte (pH = 12) and a graphite counter electrode in a H-shaped glass cuvette. Cobalt sulphide (CoS) solution is used for to sensitized the counter electrode and the counter electrode placed behind the film electrode at a distance of about 4 mm. The exposed area (1 cm²) of the active electrode was defined by an epoxy resin. The cell is lock by means of a rubber cork and contacts were taken out. In the second arm of the cell saturated calomel electrode (SCE) was placed. The whole assembly was put under the copper pot. The cell through an electrolyte solution was illuminated using a simple tungsten halogen lamp. Cell properties such as I-V characteristics in dark, barrier height, photovoltaic output (under 20 mW/cm²) characteristic and photoresponse were studied as a relation with an composition x of an electrode.

3. Results and discussion:

3.1. Film Growth and Deposition Parameters Optimization:

The Cd^{+2} , Mn^{2+} and S^{2+} ions were co-accumulated to form $Cd_{1-x}Mn_xS$ thin films in an aqueous alkaline medium (pH = 10.2), for the range of composition $0 \le x \le 0.5$. substrates for deposition were glass and stainless steel strips in a reaction container. The reaction container contain solutions of varying amount of cadmium, manganese, thiourea, aqueous ammonia and TEA.

Reactions to be proposed were as follows:

$$\begin{array}{c} \text{CdSO}_4 + 4\text{NH}_3 \longrightarrow & [\text{Cd(NH}_3)_4]^{2+} \\ \text{(1)} & \text{MnSO}_4 + 4\text{NH}_3 \longrightarrow & [\text{Mn(NH}_3)_4]^{2+} \\ \text{(2)} & \end{array}$$

The rate of growth of thin film is depends upon the pH of the solution in reaction bath and temperature of the solution in reaction bath. The deposition temperature increases from 40 to 90 °C. It has been observed that at low temperature, just above the room temperature there is no film deposition because of at low temperature all ions are in bound state , [13, 14]. The temperature of the reaction bath was increased from 40–90 °C and the terminal film thickness was measured. It is observed that the terminal film thickness increased nearly linear with the deposition temperature. The terminal film thickness maximum at around 80 °C and after 80 °C it is decreases with higher deposition temperatures [13, 14].]. The variation of film thickness with deposition temperature is shown in Figure 1.

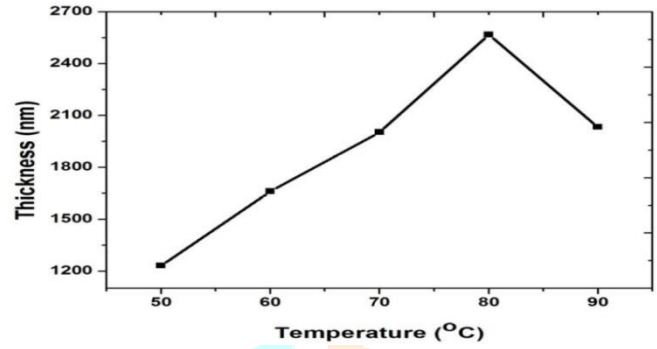


Figure 1. Variation of $Cd_{1-x}Mn_xS$ (x = 0.4) film thickness with deposition temperature, at 60 minutes,.

The next deposition parameter to be optimizes is deposition time. An appropriate deposition time is 60 min. [13, 14]. It has been found that the film deposition is time-dependent and in the beginning it is linear with higher rate of deposition and then saturates with lower rate of deposition. Figure 2. Shows the variation of film thickness as a function of deposition time for Cd1-xMnxS (x=0.4). Initially film thickness increases with deposition time reaches maximum value and then decreases. Such behavior can be understood by film formation and continuous precipitation in 2100 nm with deposition time 30-105 min. The maximum thickness 2100nm was observed for deposition time 60 min. It is observed that the film deposition rate is higher in early stage and after that deposition rate decreases with increases in deposition time. The average rate of deposition is 36.67 nm/min.

The film growth parameters such as pH of bath solution and speed of rotation of substrates are also optimized. A speed of the substrate rotation (60 rpm) was determined to obtain a maximum terminal film thickness. The pH value of reaction mixture optimized was 10.3 for maximum thickness of the films [13, 14]. The different deposition parameters and deposition conditions that were optimized are [13, 14].

- a) Deposition temperature = 80 °C;
- b) Deposition time = 60 min
- c). Reaction mixture pH = 10.2.
- d) Substrate rotation speed = 60 rpm
- e) Volume of the TEA = 3 ml,
- f) Volume of the ammonia = 14 ml

The color of CdS (x = 0) film samples are yellowish orange and the color of the other Compositions were changed slowly from yellowish orange to yellowish brown as x increased from 0 to 0.4. The change in color with the higher Mn-concentration in CdS shows that Mn2+ establish an alloy with CdS under optimized experimental conditions. Then the films were characterized compositionally by an energy dispersive analysis by x-rays technique. It has been observed that Mn²⁺ replaces Cd²⁺ and not S²⁻ [13, 14].

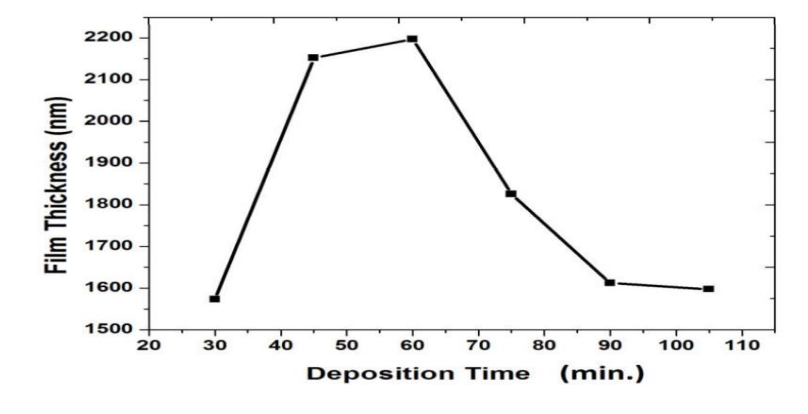


Figure 2. Film thickness as a function of deposition time for $Cd_{1-x}Mn_xS$ (x = 0.4).

i352

3.2. Compositional investigations:

The energy dispersive X-ray analysis is the basic technique useful for to know the elemental composition of the materials. The composition of Cd, Mn and S in Cd1-xMnxSthin films were recorded on energy dispersive X-Ray spectrometer attached to the scanning electron microscope. The chemically elemental compositional determination in the $Cd_{1-x}Mn_xS$ thin films, i.e. contents of Cd^{2+} , Mn^{2+} , and S^{2-} for various film structures are listed in Table 1.

Table 1.	Chemical	elemental	composition	analysis	of the	$Cd_{1-x}Mn_xS$	thin composites.
----------	----------	-----------	-------------	----------	--------	-----------------	------------------

Composition, <i>x</i>	Mn at%	Cd at%	S at%
0.0	0.0	50.10	48.90
0.10	2.70	48.80	48.50
0.20	3.64	46.33	50.03
0.30	5.35	44.72	49.93
0.40	6.82	43.28	49.90

3.3. Photonic analysis:

The semiconductor photoelectrode is placed in an electrolyte solution and is exposed to light of the correct wavelength. This causes the production of extra charge carriers due to light absorption, and these carriers are separated in the space charge regi<mark>on. In the n-type material, electrons travel deep into the material while holes</mark> move to the surface of the semiconductor, leading to a redox reaction [15 - 17]. The process of separating the charges works against the electric field, which is strongest when the cell is not connected to a circuit. This is called the open circuit photo voltage, which acts as a force pushing electrons from the semiconductor to the counter electrode, while the electrolyte takes in the holes [16–17]. The relationship between current and voltage for Cd_{1-x}Mn_xS photoelectrode cells with different compositions and a polysulfide electrolyte was studied. When the photoelectrode is placed in the electrolyte solution, the cell produces a dark voltage V_D and a dark current I_D, likely because of the difference in potential between the Cd_{1-x}Mn_xS electrode and the counter electrode [15, 18–19]. In an electrode-electrolette system, the charge transfer reaction is controlled by the Butler-Volmer relation [15–18, 19], and the symmetry factor determines the type of junction formed at the interface. The junction formed is of the rectifying type nature [15–17], analogues to the Schottky diode barrier junction. The junction diode ideality factor, nd, determines the quality of the junction. This factor was found by measuring the short-circuit current, log Isc, relative to the short-circuit voltage V_{sc} for all cell compositions. It was observed that recombination is more efficient at the electrode-electrolyte interface [16]. The junction barrier heights φB of the electrode material compositions for the cells were calculated from the temperature dependence of the reverse saturation current. As temperature increases, the saturation current changes in a nonlinear way. This behavior is attributed to the Pool-Frenkel type of conduction mechanism [18, 20]. The barrier heights are given in the Table 2. The power output curves were measured for different cells with varying electrode compositions. The cell parameters like short-circuit current (I_{sc}), open-circuit voltage (V_{oc}), efficiency (n%), and fill factor (FF%) were calculated. It was noticed that Isc and Voc increased a lot as the value of x went from 0 to 0.1, but then started to go down for higher values of x. The increase in Isc and Voc at x = 0.1might be because the electrode material had better grain structure and the cell had lower series resistance [15– 17, 20]. Figure 3 shows how the conversion efficiency (n\%) and fill factor (FF\%) depend on the electrode composition parameter x. Efficiency rises up to x = 0.1 and then drops. We think this improvement is because of the higher I_{sc} and V_{oc} in the cells.

parameters.									
Sr.N0	Electrode	Voc,	Isc	Rs,	Rsh,	η,	FF	ηd	ΦB
	Comp x	mV	μA/cm	kΩ	kΩ %	%	%	mV	eV
1	0.00	382	182	0.755	5.00	0.13	37.20	2.52	0.83
2	0.10	452	212	0.910	4.21	0.22	40.00	2.40	0.60
3	0.20	265	124	0.940	3.83	0.18	37.30	2.61	0.65
4	0.30	233	105	0.975	3.63	0.11	36.20	2.85	0.50
5	0.40	221	096	1.013	3.55	0.074	35.75	2.995	0.48

Table 2. $Cd_{1-x}Mn_xS$ lectrodes $(0.0 \le x \le 0.4)$ and electrolyte formed electrochemical cell performance parameters.

The increase in short-circuit current is probably due to lower series resistance, while the rise in open-circuit voltage is because the electrode material has better grain structure. These results are similar to what Mahapatra and Roy [22] and Deshmukh et al [14, 15, 21] found for mixed alloy materials.

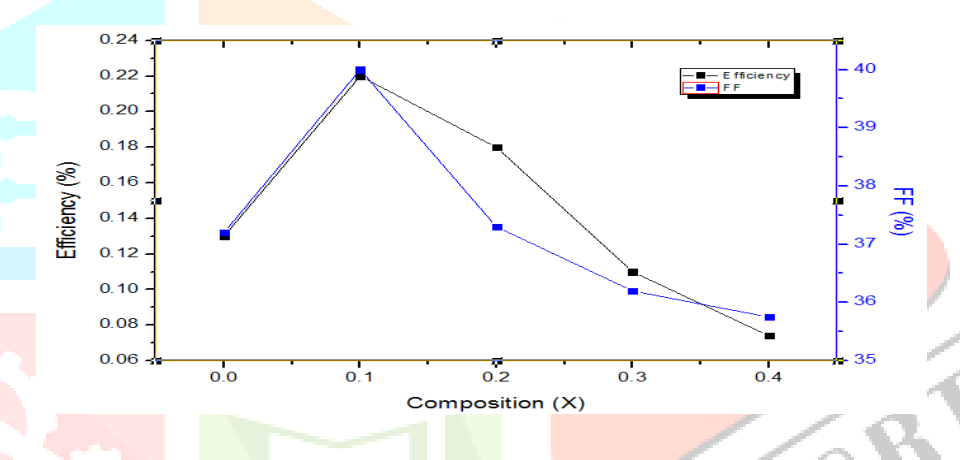


Figure 3. Variation of efficiency (η %), and fill factor (ff, %), with composition. X

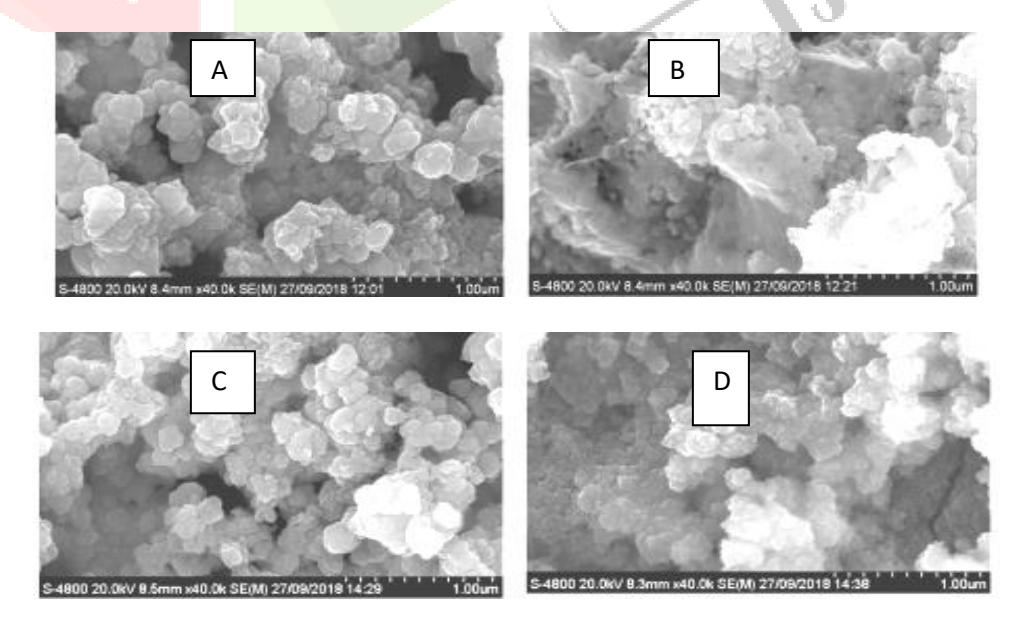


Figure 4. Shows the SEM micrographs of four typical electrode material compositions. A) x = 0.1, B) x = 0.2, C) x = 0.3 and D) x = 0.4

As the amount of 'x' increases, more Mn atoms are added into the CdS structure, which is also seen in the XRD and SEM results. It is also noticed that with an increase in 'x', there is more grain growth. This happens because the rate at which Cd and Mn ions from the solution deposit onto the substrate decreases, due to the presence of a complexing agent in the solution. This behavior has been reported by other researchers [23-25]. The Cd0.9Mn0.1S material has a very good and uniform structure. The SEM images show significant improvement in the grain structure when x is 0.1, which is also reflected in the better performance of the electrochemical cells made from this material.

4. Conclusions

Device grade and highly oriented $Cd_{1-x}Mn_xS$ ($0 \le x \le 0.4$) thin films can be made on glass using a simple and affordable chemical bath deposition method. These films can act as electrodes in photoelectrochemical cells, which help turn light into electricity. The material properties can be adjusted to work best with the full range of sunlight. In this study, among all the different compositions of $Cd_{1-x}Mn_xS$ ($0 \le x \le 0.4$), the one with x = 0.1shows the best performance in the electrochemical cell.

References:

- 1. Kariper, E. Guneri, F. Gode, C. Gumus, Chalcogenide Letters, 9(1), 27-44,2012.
- 2. R. Sankapal, R. S. Mane, C. D. Lokhande, Mater. Res. Bull., 35,177-184, 2000.
- 3. S. Venugopalam, A. Petroue, R. Galazka, A. Ramdas and S. Rodriguez, Phys. Rev., B 25, (1982), 22681.
- 4. D. Chuu, Y. Chang and C. Hsiesh, *Thin Solid Films.*, **304**, (1997), 28
- 5. C. Tsai, S. Chen, D. Chuu, and W. Chou, *Phys.*, *Review*, B **54**, (1996), 11555
- 6. D. Rodic, V. Spasojevic, A. Bajorek and P. Orinerud, J. Mag. and Mag. Mater., 152, (1996), 159.
- 7. J. Furdyna, J. Appl. Phys., R **29**, (1988), **64**
- 8. B. Jonker, X. Liu, W. Chou, A. Petrou, J. Warnock, J. Krabes and G. Prinz, J. Appl. Phys., 69, (1991), 6091.
- 9. W. Chou, A. Petrou, J. Warnock, B. Jonker, *Phys. Rev. Lett.*, **617**, (1991), 3820
- 10. C. Suryanarayanan, A. Lakhamanan, V. Subramanan and R. Kumar, Bull. Electrochem., 2, (1986), 57.
- 11. S. S. Kale, U. S. Jadhav, C. D. Lokhande, Int. J. Pure Appl. Phys., 34,324,1996.
- 12. A. Mondal, T. k. Chaudhari, P. Pramanik, Sol. Energy Matter, 7,431,1983.
- 13. V. Karande, S. Mane, V. Pujari and L. Deshmukh, Proc. *Indo-Japan Symposium On Advances In* ElectronicMaterials., Karikudi, India Nove. 2006.
- 14. E. Masumdar, V. Gaikwad, V. Pujari and L. Deshmukh, J Mat. Sci; Mat. In Elect., 14, (2003), 43.
- 15. A. Aruchami, G. Aravamudan and G. Subba Rao, Bull. Mater. Sci., 4, (1982), 48...
- 16. L. Deshmukh, *Ind. J. Pure Appl. Phys*, **36**, (1998) 302.
- 17. L. Deshmukh, A. Palwe and V. Sawant, Sol. Cells., 28, (1990), 341
- 18. J. Bockris and A. Reddy, *Modern Electrochemistry*, vol. 2 (Plenum, New York, 1973) p. 845.
- 19. K. Rajeshwar, L. Thompson, P. Sing, R. Kainthla and K. Chopra, J. Electrochem. Soc., 128, (1981), 1744.
- 20. N. Parakh and J. Garg, *Indian J. Pure Appl. Phys.*, **25**, (1987), 110.
- 21. S. Pawar and L. Deshmukh, *Mat. Chem. Phys.*, **10**, (1984), 83.
- 22. P. Mahapatra and C. Roy, *Electrochem*, *Acta.*, **29**, (1984), 1435
- 23. W. S. Seo, H. H. Jo, K. Lee, J. T. Park, Adv. Mater., 15, 795, 2003.
- 24. A. Andreev, R. Resel, d. M. Smilgies, H. Hoppe, G. Matt, H. Sitter, N. S. Saricifici, D. Meissner, H. Plank, O. Zrzavecka, Synthetic Metals, 138,59,2003.
- 25. W. Q. Han, R. Brutchery, T. D. Tilley, A. Zettl, Nano Lett. 4, 173, 2000